*Plant Ecophysiology*
https://www.sciltp.com/journals/PlantEcophys

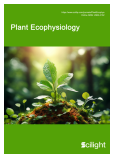

*Article*

# Assessing Freezing Tolerance in Antarctic and Arctic Plants, Lichens and Algae by Using an Innovative Freeze-Inducing and Monitoring System

Francesc Castanyer-Mallol [1,*], Miren I. Arzac [2], León A. Bravo [3,4], Marc Carriquí [1], Neus Cubo-Ribas [1], Beatriz Fernández-Marín [2,5], Jeroni Galmés [1], José I. García-Plazaola [2], Javier Gulias [1], Miquel Ribas-Carbó [1], Javier Martínez-Abaigar [6], Encarnación Núñez-Olivera [6], Luis G. Quintanilla [7] and Jorge Gago [1]

[1] Research Group on Plant Biology under Mediterranean Conditions, Department of Biology, University of the Balearic Islands (UIB), Institute of Agroecology and Water Economy (INAGEA), Carretera de Valldemossa Km 7.5, 07122 Palma, Spain
[2] Department Plant Biology and Ecology, University of the Basque Country (UPV/EHU), Barrio Sarriena s/n, 48940 Leioa, Spain
[3] Department of Agronomic Sciences and Natural Resources, Faculty of Agricultural Sciences and Environment, University of La Frontera, Ave. Francisco Salazar 01145, Temuco 4811230, Chile
[4] Network for Extreme Environment Research (NEXER), Scientific and Technological Bioresource Nucleus (BIOREN), University of La Frontera, Ave. Francisco Salazar 01145, Temuco 4811230, Chile
[5] Department Botany, Ecology and Plant Physiology, University of La Laguna (ULL), 38200 La Laguna, Spain
[6] Facultad de Ciencia y Tecnología, Universidad de La Rioja, Madre de Dios 53, 26006 Logroño, Spain
[7] Global Change Research Institute, University Rey Juan Carlos, Tulipán s/n, 28933 Móstoles, Spain
* Correspondence: xisco.castanyer@gmail.com

**How To Cite:** Castanyer-Mallol F, Arzac MI, Bravo LA, Carriquí M, Cubo-Ribas N, Fernández-Marín B, Galmés J, García-Plazaola JI, Gulias J, Ribas-Carbó M, Martínez-Abaigar J, Núñez-Olivera E, Quintanilla LG & Gago J. (2025). Assessing Freezing Tolerance in Antarctic and Arctic Plants, Lichens and Algae by Using an Innovative Freeze-Inducing and Monitoring System. *Plant Ecophysiology, 1*(2), 1. https://doi.org/10.53941/plantecophys.2025.100010.

Received: 5 May 2025
Revised: 16 July 2025
Accepted: 16 July 2025
Published: 4 August 2025

Academic Editor:
Jaume Flexas Sans

**Abstract:** Assessing freezing tolerance in photosynthetic tissues is essential for understanding plant adaptation to extreme environments such as Antarctica and the Arctic. This study presents a new portable thermoelectric device capable of applying controlled thermal cycles and measuring photosynthetic efficiency ($F_v/F_m$) in situ by means of coupling with a commercial fluorometer. The device, designed for remote field studies, offers significant improvements in portability, precision, and analytical capacity compared to previous systems. It was tested in both Antarctic and Arctic environments, covering a wide taxonomic diversity including algae, lichens, bryophytes, and tracheophytes, and revealing differential patterns of freezing tolerance across groups. To explore these differences, the experimental approach included (1) nucleation temperature; (2) the maintainability of $F_v/F_m$ after a freeze-thaw cycle at different temperatures, durations, and temperature vs. time change ramps; and (3) the time-course of $F_v/F_m$ during a freeze-thaw cycle, i.e., allowing for impact vs. recovery assessment. The results show that many species tolerate subzero temperatures by maintaining photosystem II functionality even after ice formation, with tolerance varying among taxonomic groups. Antarctic lichens exhibited exceptional resistance, while vascular plants showed greater sensitivity. The device demonstrated high thermal homogeneity, reliability, and efficiency, making it a versatile tool for ecophysiological studies of photosynthetic organisms subjected to extreme conditions.

**Keywords**: Antarctic plants; Arctic plants; cryothermocycler; $F_v/F_m$ recovery; $F_v/F_m$ maintaining; freezing test; freezing tolerance; innovative device; nucleation temperature

## 1. Introduction

The adaptation of plants to extreme environments—such as polar regions, high-altitude areas, or cold deserts—has generated increasing interest in the field of plant ecophysiology. These habitats, characterized by harsh conditions—low temperatures, water scarcity, and in some cases high levels of ultraviolet (UV) radiation—pose a significant survival challenge for plant species living there (Fernández-Marín et al., 2020). Notably, some species avoid the harshest conditions through life cycle adaptations, such as

surviving freezing periods as seeds or underground storage organs (e.g., bulbs or rhizomes), thereby escaping exposure in vulnerable developmental stages (Sakai and Larcher, 1987). Here, we focus specifically on photosynthetic tissue tolerance. In this context, cold tolerance is very relevant, given that many species under these extreme conditions must endure subzero temperatures for extended periods of time (Fernández-Marín et al., 2020). It is worth noting that cold tolerance encompasses two distinct physiological responses: chilling tolerance, which refers to the ability to withstand low but non-freezing temperatures (typically between 0 °C and 15 °C), and freezing tolerance, which involves survival at subzero temperatures where ice formation can occur within tissues. Indeed, there is evidence that some plants have specific mechanisms to cope with freezing, which might be species-specific, as shown by Birkeland et al. (2022) in a comparative study of the effects of low temperatures on gene expression among three Arctic species and Arabidopsis.

Over the years, research on the capacity of plants to tolerate these multiple stresses has provided valuable insights into the underlying important survival physiological mechanisms. However, most of this research has focused on model or crop species (Adhikari et al., 2022; Wang et al., 2022; Li et al., 2024), thereby overlooking the broader plant diversity that naturally develops in these extreme environments, which is likely to reveal levels of tolerance not described for other species (Flexas et al., 2025).

Several studies on freezing tolerance have been conducted in native Arctic species (Robberecht and Junttila, 1992; Junttila and Robberecht, 1993; Körner and Alsos, 2009) and in Antarctic species (Bravo et al., 2001, 2009; Sierra-Almeida, Cavieres and Bravo, 2018; Perera-Castro et al., 2021; López, Sanhueza, et al., 2023; Andrzejowska et al., 2024). However, comparing these studies is challenging due to the considerable variability in the methods employed—both on the exposure of plants to low temperatures as well as on how to determine freezing tolerance. Over the past 60 years, many direct and indirect methods have been described to measure plant resistance to thermal stress. These methods are predominantly based on parameters such as plant survival, visual leaf damage, root regrowth, tissue viability, electrical conductivity, gas exchange, chlorophyll fluorescence, or the activity of stress-related biomolecules (Paulsen, 2002; Thalhammer and Hincha, 2014; Geange et al., 2021). Among all these protocols, chlorophyll fluorescence is one of the most widely employed, with the parameter maximum photochemical efficiency of PSII ($F_v/F_m$) being the most frequently used. $F_v/F_m$ is considered a proxy for the physiological condition of the plant and reflects the status of the photosystem II (PSII) complex, a central player in photosynthesis and a highly thermosensitive structure (Chaudhary et al., 2020). Although several other parameters related to PSII activity have been described—e.g., photosynthetic quantum efficiency (φPSII), electron transport rate (ETR), non-photochemical quenching (NPQ), and the vitality index (Rfd) (Maxwell and Johnson, 2000; Perera-Castro et al., 2018)—$F_v/F_m$ remains the most commonly used parameter in thermosensitivity studies. It should be noted that $F_v/F_m$ can also decrease in response to low temperatures as a result of acclimation via sustained down-regulation of photosynthesis (Norman, Huner and Fathey, 1998).

Traditionally, thermal stress induction in photosynthetic organisms has been performed using devices such as refrigerators, freezers, ovens, water baths, or controlled growth chambers. While these devices allow for the regulation of exposure temperature, they are not easily transportable and are therefore inefficient for fieldwork. Their large size and weight, along with high energy consumption, make their use outside the laboratory very challenging. Moreover, these methods typically lack precise controls to apply temperature gradients that mimic actual environmental conditions, and their range of applicable temperatures is often limited. The lack of adequate equipment for these studies is clearly revealed in a review by Geange et al. (2021) that examined 3743 experiments reported in 1691 scientific articles, showing that 94% of these experiments were conducted using temperature-controlled growth chambers or water baths. This high reliance on traditional devices highlights the limited innovation in this area, as well as the need to develop advanced methods to overcome the aforementioned technical limitations. Thus, the study of thermal stress tolerance in photosynthetic organisms from habitats subjected to extreme temperatures would require the development of portable devices capable of performing in situ measurements.

In this regard, the device presented by Arnold et al. (2021) and later used by Harris et al. (2023) and Danzey et al. (2024) offers significant advantages due to its portability and its ability to cool a large number of samples simultaneously. It operates through cooling via Peltier elements attached to an aluminium thermal plate, where samples are placed and monitored by chlorophyll fluorescence measurements. Overall, it is a highly efficient method to induce thermal stress by exposing leaves to controlled thermal cycles and assessing their stress by measuring chlorophyll fluorescence to determine their critical thermal limits. This approach represented a significant step-forward in characterizing the stability of photosystem II (PSII) under thermal stress conditions.

Here we present a portable device based on a similar principle, introducing several modifications (Patents ES 2 960 435 A1 and WO/2024/028532 A1) designed to enhance its performance under remote field conditions. This device was already briefly used and mentioned, but not described, in Arzac et al. (2024). Two experiments were conducted to evaluate the effectiveness of the device in both Antarctic and Arctic photosynthetic organisms (from algae to tracheophytes). In addition, the reliability and versatility of the instrument is discussed. Given that we have used photosynthetic organisms belonging to very different evolutionary lineages, and for the sake of brevity, we will overall refer them as “plants” from now on. In summary, the freezing tolerance of the organisms used, as estimated with the new method, matches well with inter-specific differences previously described using pre-existing methods.

## 2. Materials and Methods

### *2.1. A new device for inducing freezing in plant samples*

Similarly to the device used by Arnold et al. (2021), the present instrument is based on a thermal plate with temperature regulated by Peltier elements, with several design modifications (Figure 1 and Supplementary Material S1). On top of the thermal plate, there is an interchangeable aluminium thermal block designed to accommodate samples of different sizes and compositions (solid or liquid). The device incorporates a multi-material lid, designed to optimize thermal stability and system efficiency. This lid consists of a metallic base in direct contact with the thermal block, ensuring a homogeneous temperature distribution across the samples. On top of this metallic base, there is a 40 mm layer of high-density extruded polystyrene and wood insulation, which extends over both the upper and lateral sections of the lid. Finally, a second metallic layer covers the entire structure, providing additional protection. This design modification enables the samples to be exposed to temperatures below −20 °C, independently of the external temperatures (Table 1, for details). Additionally, the lid design eliminates condensation and minimizes sample dehydration, a phenomenon that has been repeatedly observed in practice. It has been noted that samples sealed quickly in the wells remained hydrated after a complete freezing-recovery cycle, whereas those left exposed for a longer period before sealing showed signs of dehydration. Thanks to this improvement, the use of wet paper, previously employed in the device described in Arnold et al. (2021), can be omitted, thereby preventing potential adverse effects on the measurement, such as its influence on nucleation and on freezing resistance. A short description of our instrument is shown in Figure 1 and a complete comparison of our instrument with the device described by Arnold et al. (2021) is presented in Table 1. These modifications include the ability to expose samples to thermal cycles as low as −20 °C under ambient laboratory conditions, without requiring an external controlled cold environment, as well as ensuring their compatibility with a Junior-PAM measuring device (Heinz Walz GmbH, Effeltrich, Germany), which is relevant for three main reasons: first, because this device uses thin optical fibers that allow the sample wells to be sealed; second for comparative reasons, as it is the one used by our research group to evaluate dehydration tolerance in photosynthetic organisms (López-Pozo et al., 2019) and ultraviolet (UV) radiation tolerance (pending publication); and third, due to its easy portability, making it ideal for studies in remote locations.

**Table 1.** Comparison between the instrument described in Arnold et al. (2021) and the one used in the present study.

| | **(Arnold et al., 2021)** | **ES 2 960 435 A1** |
|---|---|---|
| Measurement unit | **Maxi-Imaging-PAM**<br>☒ Hardly portable<br>☒ Expensive<br>☒ High power consumption (9W)<br>☒ Delicate optical components<br>☑ Multiple samples at once | **Junior-PAM**<br>☑ Highly portable<br>☑ Affordable<br>☑ Low power consumption (500mW)<br>☑ Robust, simple fiber optics<br>☒ Single sample measure at a time per fiber optic |
| Number of samples | ☑ Up to 30 whole leaves<br>☑ Up to 68 discs<br>☒ Not designed for liquid samples | ☑ Up to 30 whole leaves (or photosynthetic organs)<br>☑ Up to 68 discs<br>☑ Up to 68 liquid samples |
| Method to prevent dehydration | ☒ Wet paper<br>(may affect nucleation point and accuracy) | ☑ Sealed well<br>(moisture remains stable) |
| Peltier control software | **LabView**<br>☒ Proprietary and paid<br>☒ Limited to a single platform (Windows)<br>☒ Low performance<br>☒ Small community and limited support<br>☒ No integration with cloud services<br>☒ Restricted to a single programming language<br>☑ Specialized environment for data acquisition<br>☒ Dependence on National Instruments' ecosystem | **Microsoft .NET open-source platform**<br>☑ Open-source and free<br>☑ Cross-platform<br>☑ High performance<br>☑ Large community and support<br>☑ Integration with cloud services<br>☑ Compatibility with multiple languages<br>☒ Not a specialized environment for data acquisition<br>☒ Dependence on Microsoft's ecosystem |
| Minimum and maximum temperature cycles | **−20 to 100 °C**<br>☒ Insulation made with double glass thermopanel | **−30 to 100 °C**<br>☑ Insulation through a main lid specially designed to prevent thermal load from the environment and prevent sample dehydration |
| Minimum temperature at 20–22 °C ambient | ☒ −14 °C | ☑ −25 °C |
| Minimum temperature at 4 °C ± 2 °C ambient | ☒ −20 °C | ☑ −30 °C |

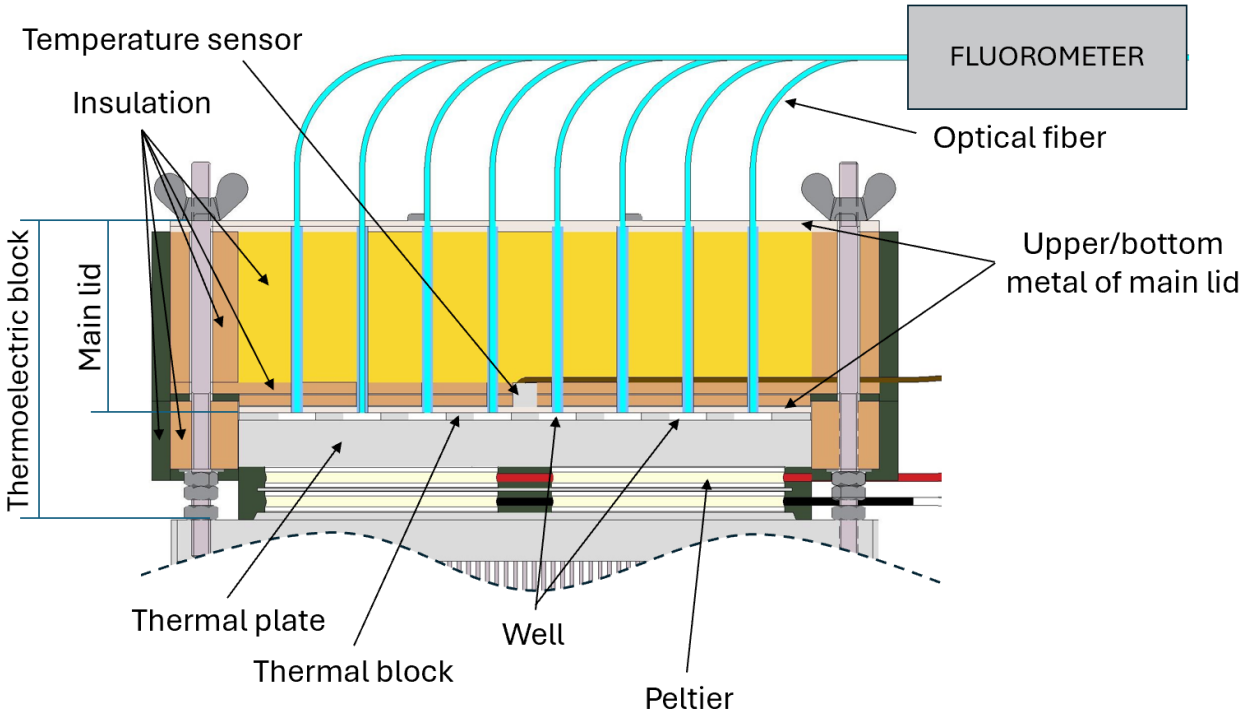


**Figure 1.** Schematic of the thermoelectric block and its main components. The thermoelectric block consists of Peltier elements, thermal plate, thermal block, and main lid. The thermal block contains the wells that hold the samples. The main lid is composed of a thick insulating layer covered on top and bottom sides by metal sheets. The bottom sheet also serves as the metallic lid that seals the wells where the samples are placed. Inside the main lid, in direct contact with the bottom metal sheet, there is a temperature sensor, which, when connected to the control system, enables the reproduction of programmed thermal cycles. Additionally, optical fibers are included to facilitate the measurement of the maximum photochemical efficiency of PSII in photosynthetic organisms by connecting to a fluorometer. A detailed description of the instrument is provided in Supplementary Material S1.

### *2.2. Verification of the device's thermal homogeneity*

Thermal homogeneity of the device, defined as the uniform distribution of temperature across different points under various experimental conditions, was assessed using eight type K thermocouples 0.13 mm diameter, model TL0260 (PerfectPrime, n.d.) connected to a Campbell CR1000X data logger (Campbell Scientific Inc., Logan, UT 84321, USA).

Three experimental setups were designed to evaluate thermal homogeneity across the thermal block by analysing the temperature at eight wells (Supplementary Material S2, Figure S2.1), assessing both Top and Bottom temperatures. In the first setup, a low-density polyethylene (LDPE) sheet (0.2 mm) was placed between the thermal plate and the thermal block, acting as a thermal diffuser. In this case, two measurements were performed: one on the surface of the polyethylene sheet (at the bottom of the wells) and another on the lower stainless-steel plate of the main lid covering the wells (top of the wells). In the second setup, the polyethylene sheet was removed, and measurements were taken directly on the thermal plate and, again, on the lower stainless-steel plate of the main lid. Finally, in the third setup, thermocouples were attached to paper discs (80 g $m^{-2}$) allowing an assessment of thermal homogeneity under conditions closer to experimentation with photosynthetic organisms. Temperatures were recorded every 30 s for detailed monitoring, with the standard error of each thermocouple relative to the set-point temperature being analysed.

To evaluate the effectiveness of the device, several experiments were conducted in two polar regions—the Antarctic (South Shetland Islands) and the Arctic (Svalbard Islands)—as examples of remote environments. In the Antarctic region, two experiments were performed (Experiments 1A and 1B). Experiment 1A focused on assessing the nucleation temperature of photosynthetic tissues from various local species, while Experiment 1B evaluated the capacity to maintain PSII efficiency following a controlled freeze-thaw cycle. In the Arctic region, Experiment 2 was conducted with tracheophytes and included both the assessment of the capacity to maintain PSII efficiency during the freeze-thaw cycle and the estimation of recovery capacity. The latter was inferred by inserting an additional $F_v/F_m$ measurement at the end of the minimum target temperature period during the freeze-thaw cycle. Additionally, thermal homogeneity of the device was assessed in the Antarctic location.

### *2.3. Chlorophyll fluorescence measurements*

Chlorophyll fluorescence measurements were performed using a Junior-PAM fluorometer (Heinz Walz GmbH, Effeltrich, Germany). This compact and portable device is designed for teaching and basic research on plant photosynthesis. It employs Pulse-Amplitude Modulation

(PAM) fluorometry to assess photosystem II efficiency, providing valuable insights of plant photosynthetic performance and health. The blue light version, equipped with a 445 nm peak-emission LED, is suitable for most eukaryotic algae and tracheophytes and was used to measure $F_v/F_m$ in experiments 1B and 2, using samples previously acclimated to darkness. The instrument is equipped with 1.5 mm diameter plastic optical fibers that fit perfectly into the main lid of the device. This setup seals the sample wells, preventing water loss and enabling accurate chlorophyll fluorescence measurements. It is powered and controlled via a USB port.

### *2.4. Experiment 1. Freezing tolerance in Antarctic species*

The first experiment was conducted at the Spanish Antarctic Base Juan Carlos I (BAE JCI). BAE JCI is located on the Hurd Peninsula of Livingston Island, part of the South Shetland Islands archipelago (62°49′46″ S, 60°23′20″ W, 12 m a.s.l.). Situated on the southeastern coast of South Bay, approximately 200 m from the shoreline, the base is surrounded by glaciers and is set in rugged terrain with bioclimatic conditions typical of maritime Antarctica. Vegetation on the Hurd Peninsula is limited and primarily composed of non-tracheophyte species adapted to cold and desiccation, including liverworts, mosses, lichens, and algae, which colonize rocky surfaces and nutrient-poor soils. The absence of trees and shrubs characterizes this region, where low temperatures and strong winds restrict tracheophyte growth, with *Deschampsia antarctica* E.Desv. (Poaceae) and *Colobanthus quitensis* (Kunth) Bartl. (Caryophyllaceae) being the only species present. In addition to the harsh climatic conditions, biogeographic factors—such as historical isolation, limited dispersal opportunities, and past glacial events—may also contribute to this limited tracheophyte diversity (Peat, Clarke and Convey, 2007).

Samples were collected near BAE JCI immediately before the start of each experiment in order to minimize alterations in their physiological properties.

Between 17 February and 15 March 2022, various Antarctic flora species were collected (Supplementary Material S3), including algae, lichens, mosses, and tracheophytes. For each species, six specimens (n = 6) were randomly selected, from which sufficient photosynthetic tissue was gathered to cover a minimum circular area of 5 mm in diameter for each of the three thermal treatments (−6 °C, −12 °C, and −18 °C). That is, three tissue samples were obtained from each of the six specimens, with each sample simultaneously subjected to a different thermal treatment. Samples were collected near BAE JCI immediately before the start of each experiment in order to minimize alterations in their physiological properties. The time between collection and measurement never exceeded four hours. During this period, samples were kept under ambient cold conditions with approximately 100% relative humidity to preserve their physiological state.

#### Experiment 1. A. Nucleation temperatures

Nucleation temperature ($T_{nuc}$) is a key parameter in plant freezing biology, as it determines the point at which water in plant tissues start crystallization. This phenomenon can occur homogeneously at extremely low temperatures (~−38.5 °C) or heterogeneously, facilitated by internal or external particles within the plant, generally between −1.9 and −3.3 °C depending on species and environmental conditions (Pearce, 2001; Ralser, Stegner and Neuner, 2024). Measuring nucleation temperature is crucial for understanding freezing tolerance in plants, as it determines its ability to delay ice formation and minimize cellular dehydration damage. Under natural conditions, multiple factors influence nucleation, including ice-nucleating bacteria, intracellular compounds, and plant tissue structure (Ralser, Stegner and Neuner, 2024). In this context, nucleation temperatures were analysed in 17 out of the 32 species studied in Antarctica, including algae, lichens, mosses, and tracheophytes, with six replicates (i.e., specimens) per species.

A type-K thermocouple, 0.13 mm in diameter model TL0260 (PerfectPrime, n.d.), was placed on the thermal block of the cryothermocycler and used as a reference, while six identical thermocouples were inserted through the intended openings in the device lid, designed for optical fiber passage. Upon closing the cryothermocycler, these thermocouples established direct contact with each plant tissue and measured temperature every second.

In the six wells corresponding to the thermocouples inserted through the lid, the six independent specimens of each species were placed. The lid was then secured in its measuring position. Once the setup was ready, the cryothermocycler was activated with a temperature reduction program (Figure 2A). The program was setup to maintain samples at 15 °C for 30 min, a temperature previously reported to be close to optimal for the physiological activity of Antarctic bryophytes (Perera-Castro et al., 2021). After this initial stabilization phase, temperature decreased at a rate of −30 °C per hour from 15 °C to 0 °C, and then at −8 °C per hour from 0 °C to the target temperature in the case of terrestrial plants. For algae, the initial temperature was set at 5 °C (Wienckel and Dieck, 1990) instead of 15 °C. Simultaneously, a CR1000X data logger (Campbell Scientific, Inc., Logan, UT 84321, USA) recorded thermocouple values every second, once the reference thermocouple temperature was below 2 °C.

The data obtained were processed by subtracting the reference temperature from the recorded temperature of each replicate, generating a differential graph (Figure 2B, grey line) that identifies nucleation temperature precisely at the point where the exothermic peak appears, resulting from the heat release associated with the phase transition.

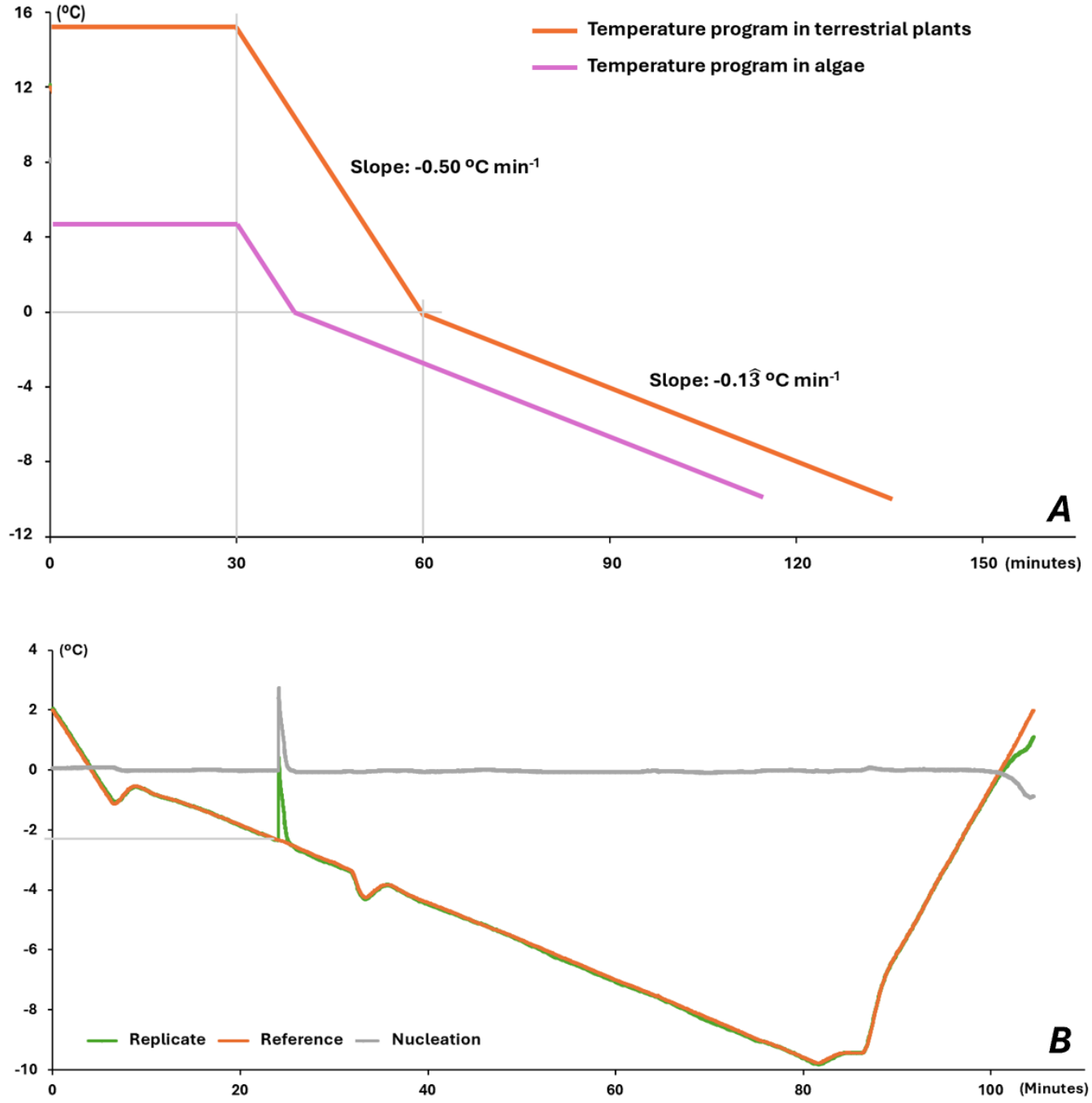


**Figure 2.** (**A**) Cooling programmes used in the nucleation assays. Terrestrial-plant samples (orange) were held at 15 °C for 30 min and then cooled at −0.50 °C $min^{-1}$ to 0 °C, followed by −0.13 °C $min^{-1}$. Algal samples (purple) followed the same ramp after an initial 30 min plateau at 5 °C. (**B**) Representative output of a nucleation experiment. The temperature of the sample (green) and of the reference thermocouple in the thermal block (orange) are plotted together with their differential (grey). The sharp positive peak marks the exothermic release of latent heat during the liquid-to-ice phase transition; the onset of this peak is taken as the ice-nucleation temperature of the sample.

Experiment 1. B. Capacity for maintaining PSII efficiency after a controlled freeze-thaw cycle

Three cryothermocycler devices were used to expose samples to three thermal treatments (−6 °C, −12 °C, and −18 °C). The organ's capacity to maintain PSII efficiency was determined by measuring $F_v/F_m$ just before $(F_v/F_m)_i$ and eleven hours after $(F_v/F_m)_f$ exposure to the thermal cycle, using samples previously acclimated to darkness for at least 30 min. The capacity for maintaining $F_v/F_m$ after a controlled freeze-thaw cycle was calculated using the following formula (Figure 3, for details):

$$\text{Capacity to maintain } F_v/F_m\ (\%) = 100 - \left(\frac{(F_v/F_m)_i - (F_v/F_m)_f}{(F_v/F_m)_i}\right) \times 100$$

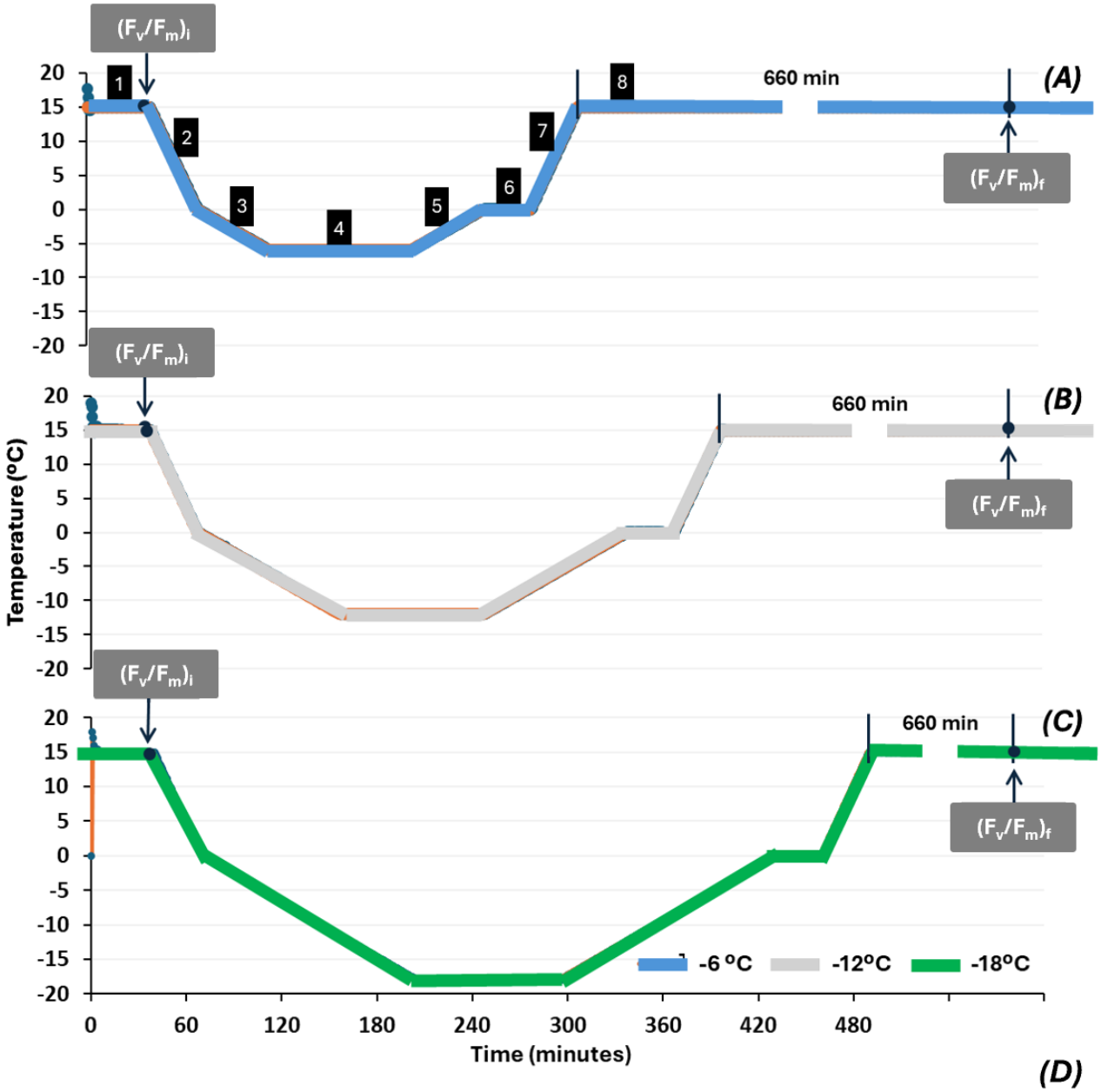


| Step | Description | Step | Description |
|---|---|---|---|
| 1 | Stabilization time at 15 °C (30 min) | 5 | Heating up to 0 °C (0.1$\hat{3}$ °C/min) |
| 2 | Cooling to 0 °C (-0.50 °C/min) | 6 | Holding at 0 °C (30 min) |
| 3 | Cooling to setpoint temp. (-0.1$\hat{3}$ °C/min) | 7 | Heating up to 15 °C (0.50 °C/min) |
| 4 | Holding at setpoint temp. (90 min) | 8 | Recovery period (660 min) |

**Figure 3.** Thermal cycles applied in each treatment and $F_v/F_m$ measurement points for each condition. (**A**) Thermal cycle applied in the −6 °C treatment. (**B**) Thermal cycle applied in the −12 °C treatment. (**C**) Thermal cycle applied in the −18 °C treatment. (**D**) (table) Specific characteristics of each period.

Each thermal block was designed to accommodate six replicates per species for 10 species. After the main lid was closed, a freeze-thaw cycle was initiated (Figure 3, for details), starting at 15 °C (Perera-Castro et al., 2021), then progressively decreasing to the target temperature of the assigned treatment, and then returning to 15 °C, where it remained until the conclusion of the experiment. For algae measurements, the cryothermocycler devices were pre-cooled to 5 °C (Wienckel and Dieck, 1990) before inserting samples. Thereafter, the same protocol was followed, although final temperature was 5 °C. A detailed description of the experimental procedure, sample handling, and cryothermocycler device preparations can be found in Supplementary Material S4.

### *2.5. Experiment 2: Freezing tolerance in Arctic species*

Similar trials to Experiment 1B were conducted in the Arctic locality of Longyearbyen, Svalbard Archipelago (78°13′ N, 15°38′ E, 50 m a.s.l.) to evaluate the capacity to maintain PSII efficiency and, in this case, also the recovery capacity of 14 species (Supplementary Material S3 for details).

Located on Spitsbergen Island, Longyearbyen is the capital of the Svalbard Archipelago, situated in Longyeardalen Valley, on the southeastern coast of Adventfjord, a fjord connected to Isfjorden, (Stange, 2018). The region is characterized by an Arctic environment, with a landscape dominated by mountains, glaciers, and permafrost-covered terrain. Vegetation in Longyearbyen is scarce, consisting mainly of Arctic tundra, with species including mosses, lichens, and some tracheophytes adapted to low temperatures and nutrient-poor soils. The absence of trees is a defining characteristic of the Arctic region, where permafrost and extreme climatic conditions limit woody plant growth (Stange, 2018). However, in sheltered areas, small patches of denser vegetation can be found.

Between 25 and 28 July 2022, various representative Arctic tracheophyte species were collected in Longyearbyen, and the same protocol described in Experiment 1B was applied, with two modifications. First, the −6 °C treatment was replaced with −9 °C, as this temperature was considered closer to the tolerance limit of tracheophytes, providing more relevant information on cold resistance (Sakai and Larcher, 1987). Consequently, the thermal cycle duration was adjusted accordingly. Second, $F_v/F_m$ was measured in all replicates at the end of the minimum target temperature period, just before the temperature started to increase back to 15 °C. This additional measurement $(F_v/F_m)_m$ allowed the recovery of $F_v/F_m$ to be assessed by comparing its value at the end of the freezing period with that upon recovery to 15 °C.

### *2.6. Statistical Analysis*

Evaluation of the effectiveness of the thermal treatments on the maintaining of $F_v/F_m$ was evaluated for each species. First, the normality of each dataset was assessed using a Shapiro-Wilk test, and the homogeneity of variances was verified using a Levene test (car package; Fox & Weisberg, 2019). In cases where both assumptions were met, a one-way ANOVA was applied for each species considering thermal treatment as a fixed factor; otherwise, the non-parametric Kruskal-Wallis test was used. When ANOVA detected significant differences, a Tukey HSD test was performed for post-hoc comparisons. In cases where Kruskal-Wallis test indicated significant differences, a post-hoc grouping analysis was performed using the Kruskal function from the *agricolae* package (de Mendiburu, 2021), which assigns treatments into homogeneous groups.

For nucleation tests, normality and homogeneity of variances were met, allowing the use of a one-way ANOVA to determine whether significant differences existed among species in terms of their nucleation temperature. When the ANOVA results indicated significant differences, a Tukey HSD post-hoc test was performed to identify specific differences among species, grouping them into statistically homogeneous subsets.

To evaluate the effects of freeze-thaw treatments on $F_v/F_m$ across three time points (initial, medium, and final), during the analysis of the recovery capacity of photosynthetic tissues of Arctic plants, a repeated measures analysis was performed independently for each species. First, the assumptions of normality and homogeneity of variances were tested using the Shapiro–Wilk and Levene's tests (car package; Fox & Weisberg, 2019). When both assumptions were met, a repeated measures ANOVA was conducted using a linear mixed-effects model (*nlme* package; Pinheiro et al., 2023), considering the individual replicate as a random factor. Post-hoc comparisons among time points were performed using Tukey's HSD tests (*emmeans* package; Lenth, 2023) and the *multcomp* package (Hothorn, Bretz, & Westfall, 2008). If the assumptions were not satisfied, the non-parametric Friedman test was applied, followed by pairwise Wilcoxon tests with Holm's adjustment for multiple comparisons, and grouping of time points based on the *multcompView* package (Graves et al., 2019).

All statistical analyses were conducted using RStudio (Version 2024.12.1 Build 563). A significance level of $p < 0.05$ was adopted for all statistical tests.

## 3. Results

### *3.1. Thermal homogeneity of the device*

Thermal block homogeneity, measured relative to the setpoint temperature (ST) at various key points (Supplementary Material S2), ensures experimental reproducibility and guarantees that all samples remain under very similar conditions. Temperature variation across the thermal block showed a maximum standard deviation value of ±1.21 °C around the setpoint temperature (Table 2).

Thermal homogeneity measured directly on a cellulose paper sheet and without the polyethylene layer, replicating Experiments 1B and 2, also provided values that ensure remarkable repeatability and thermal uniformity across different experiments, samples, and replicates.

### *3.2. Nucleation temperature in Antarctic species*

Nucleation temperature (Figure 4) was assessed in several species sampled at BAE JCI. Significant differences in nucleation temperatures among species were observed, with values varying from −6 °C to −2 °C. Among the species evaluated, *Palmaria decipiens* (Reinsch) R.W.Ricker exhibited the lowest nucleation temperature (−6 °C), while *Brachytecium austrosalebrosum* (Müll.Hal.) Kindb. had the highest value (−2 °C).

**Table 2.** Standard deviation values (in °C) obtained for each thermocouple based on its location (Supplementary Material S2) under the different experimental scenarios evaluated. Values are referenced to the setpoint temperature (ST) (see "Thermal Homogeneity of the Device" in the Materials and Methods section). Low density Polyethylene film (LDPE).

| | **Thermocouple Placement** | | | | |
|---|---|---|---|---|---|
| | **On thermal Plate** | | **Metallic Base of the Lid (in Direct Contact with the Thermal Block)** | | **On Paper Disc** |
| Thermocouple | Without LDPE (°C) | With LDPE (°C) | Without LDPE (°C) | With LDPE (°C) | Without LDPE (°C) |
| 1 | ST ± 0.435 | ST ± 0.732 | ST ± 0.833 | ST ± 0.396 | ST ± 0.706 |
| 2 | ST ± 0.745 | ST ± 0.958 | ST ± 0.318 | ST ± 0.700 | ST ± 0.243 |
| 3 | ST ± 0.710 | ST ± 0.673 | ST ± 1.002 | ST ± 0.668 | ST ± 0.927 |
| 4 | ST ± 0.636 | ST ± 0.655 | ST ± 0.950 | ST ± 0.597 | ST ± 0.889 |
| 5 | ST ± 0.544 | ST ± 0.647 | ST ± 1.013 | ST ± 0.503 | ST ± 1.170 |
| 6 | ST ± 0.564 | ST ± 0.659 | ST ± 1.212 | ST ± 0.523 | ST ± 0.837 |
| 7 | ST ± 0.486 | ST ± 0.464 | ST ± 0.840 | ST ± 0.443 | ST ± 0.792 |
| 8 | ST ± 0.415 | ST ± 0.838 | ST ± 0.694 | ST ± 0.372 | ST ± 0.642 |
| Mean | ST ± 0.567 | ST ± 0.703 | ST ± 0.858 | ST ± 0.525 | ST ± 0.776 |

### *3.3. Capacity for maintaining PSII efficiency after a controlled freeze-thaw cycle (Experiments 1B and 2)*

The percentage of Antarctic and Arctic species that maintained their $F_v/F_m$ above 85 % of their initial value after the freeze-thaw cycle decreased with the temperature treatment, being 59 %, 38 % and 30 %, at −6/−9 °C, −12 °C and −18 °C, respectively (Figure 5), demonstrating a progressive impact of decreasing temperatures on the photochemical efficiency of PSII.

Regarding Antarctic organisms, several algal species from different phyla were analysed, although the limited number of representatives of each group analysed prevents drawing definitive conclusions. Nevertheless, combining the entire algae group, more than 66 % maintained up to 85 % of $F_v/F_m$ at −6 °C and −12 °C. In contrast, only 28 % of the species subjected to −18 °C were able to maintain high $F_v/F_m$ values. Regarding lichens, they were able to maintain $F_v/F_m$ above 85 % of their maximum in all the treatments. Bryophytes, the most represented group in our survey, showed lower PSII freezing tolerance than lichens. Although above 84 % of moss species subjected to −6 °C maintained over 85 % of their initial $F_v/F_m$ levels, this percentage dropped to 46 % at −12 °C and 30 % at −18 °C. Finally, the two tracheophyte species present in the study areas also maintained more than 85 % of $F_v/F_m$ at −6 °C, but none reached these levels at −12 °C and −18 °C.

Among the tracheophyte species investigated in the Arctic, only *Papaver dahlianum* Nordh. and *Saxifraga cespitosa* L. maintained 85 % and 74 % of their initial Fv/Fm values, respectively, after exposure to −9 °C. All other species showed lower values at this temperature, and none maintained such high $F_v/F_m$ at −12 °C or −18 °C.

### *3.4. Recovery capacity of Arctic photosynthetic tissues under a controlled freeze-thaw cycle*

While experiments in Antarctica analysed the resistance of several species to low temperatures by measuring $F_v/F_m$ before and after a freeze-thaw cycle, the results raised an interesting question. Are resistant plants just keeping their $F_v/F_m$ high, or is it affected by freezing and then recovering during thaw? And, if so, what is the magnitude of this recovery?

Thus, in the subsequent experiments in the Arctic, $F_v/F_m$ was not only measured at the start and the end of the freeze-thaw cycle but also at the end of the freezing period, just before the minimum target temperature began to increase. This additional $F_v/F_m$ measurement would allow us to discern whether the final values observed were the consequence of a given maintenance of PSII during the entire freeze-thaw cycle or to a decrease during freezing followed by some degree of recovery after low temperature was removed and tissue returned to 15 °C. In general, freezing induced a decrease in $F_v/F_m$ that was only partially recovered after warming to ambient temperature (Figure 6). However, other patterns were also observed. For instance, in some species, no recovery could be observed, as there were non-significant differences between their $F_v/F_m$ values during freezing and after restoring ambient temperature. Other species (*Cerastium alpinum* L., *Dryas octopetala* L., *Equisetum arvense* L. and *Salix polaris* Wahlenb.) even exhibited significantly higher $F_v/F_m$ values during freezing at −9 °C than after restoring ambient temperature. Interestingly, *S. cespitosa* and *P. dahlianum,* did not exhibit significant differences between $F_v/F_m$ before freezing and at the end of the freezing period at- 9 °C (Figure 6A). However, this pattern was inexistent for any species at −12 °C and −18 °C (Figure 6B,C).

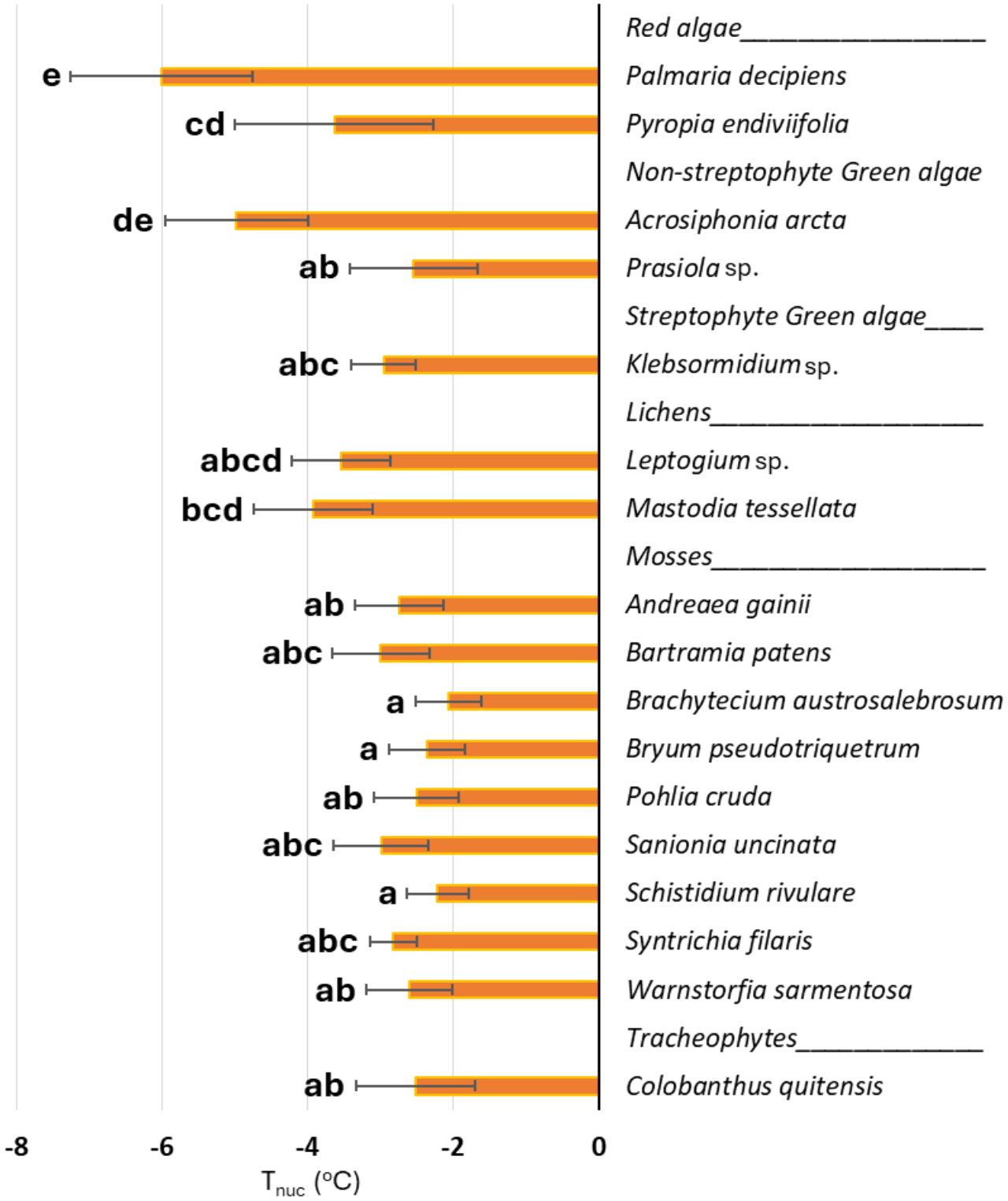


**Figure 4.** Nucleation temperature values (°C) obtained across the studied species. Bars represent the mean ± SD (n = 6 replicates per species). Different letters indicate significant differences ($p < 0.05$) according to Tukey HSD post-hoc test. Error bars correspond to the standard deviation of the measurements for each species.

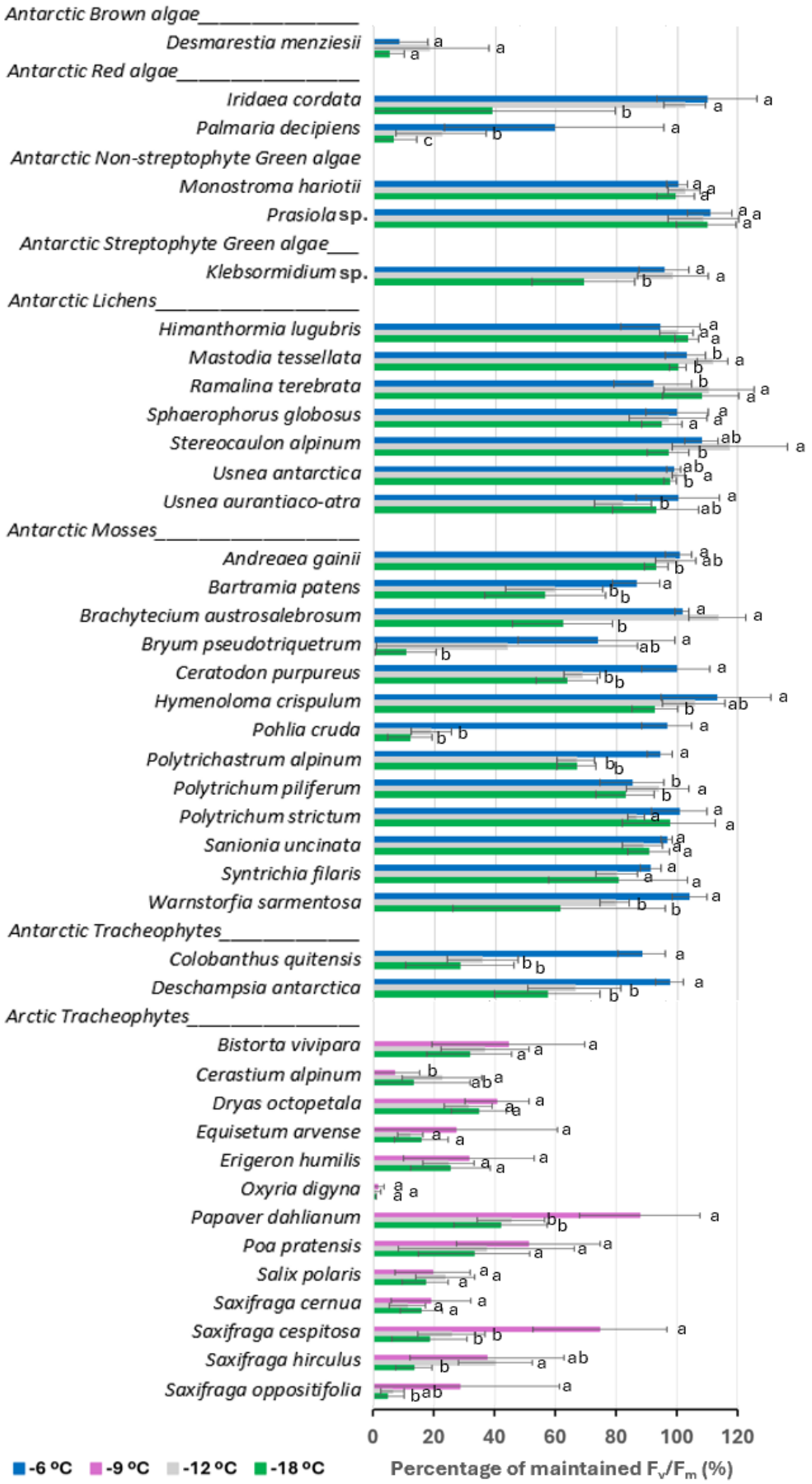


**Figure 5.** Percentage of maintained maximum photochemical efficiency ($F_v/F_m$) for each Antarctic and Arctic species under different temperature treatments: −6 °C (blue), −9 °C (purple), −12 °C (grey) and −18 °C (green). Bars represent the mean ± SD (n = 6 replicates per species). Different letters indicate significant differences ($p < 0.05$) according to the post-hoc test applied. Error bars correspond to the standard deviation of the measurements for each treatment and species.

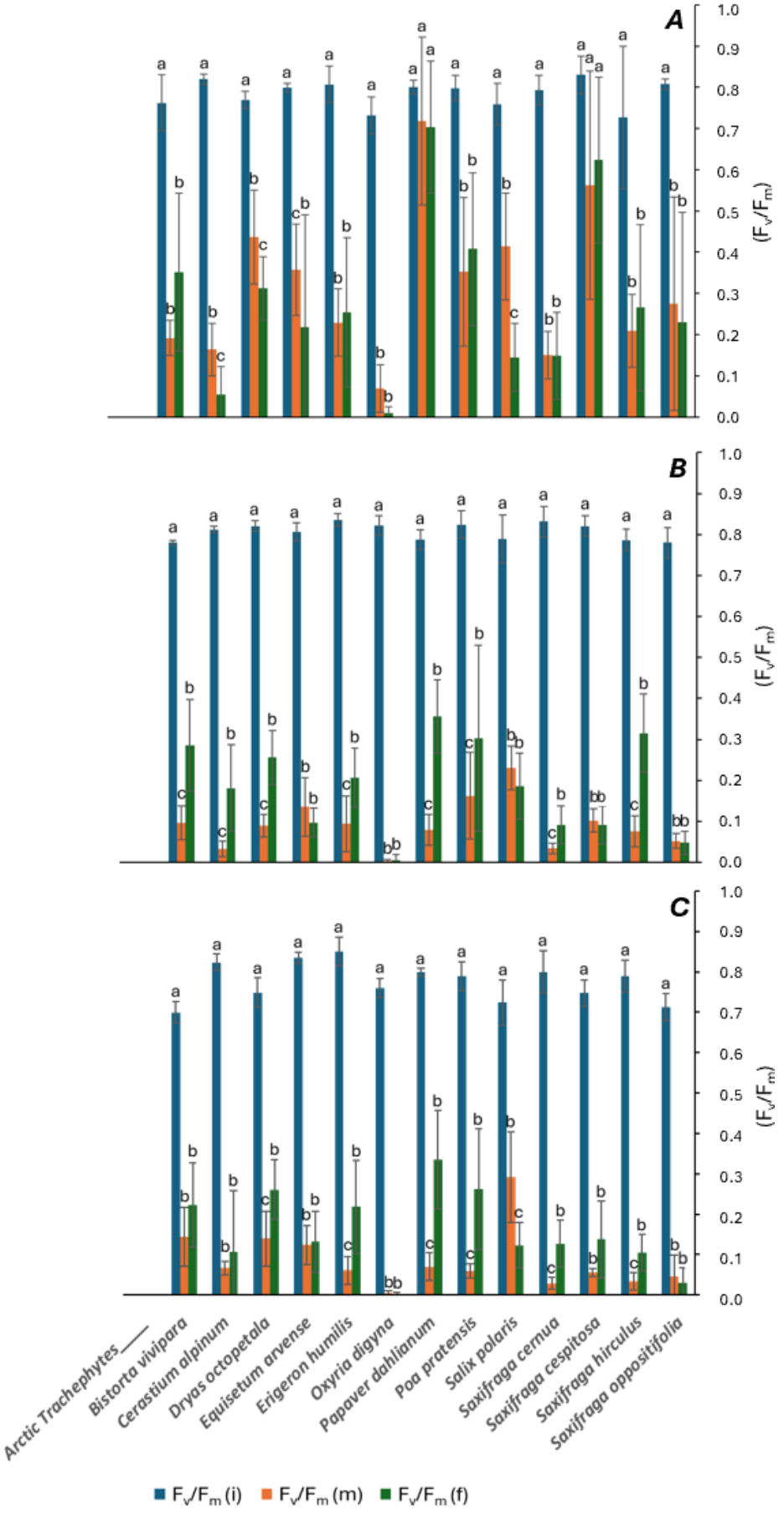


**Figure 6.** $F_v/F_m$ measurements in several Arctic species at three stages of the freeze–thaw cycle: Initial (i, blue bars), measured at the beginning of the cycle; Medium (m, orange bars), at the end of the freezing period; and Final (f, green bars), eleven hours after the end of the cycle. Plots **A**–**C** correspond to treatments at −9 °C, −12 °C, and −18 °C, respectively. Each bar shows the mean ± standard deviation (n = 6 replicates per species). Different letters indicate significant differences ($p < 0.05$).

## 4. Discussion

### *4.1. Versatility of the device used for assessing freezing tolerance*

The utility of a new device to assess the freezing tolerance of photosynthetic tissues has been tested with two preliminary assessments –one in Antarctica in January–March 2022 and another in the Arctic in July–August 2022. While recognizing the preliminary nature of these results, the usefulness of the instrument was largely confirmed. First, as shown in Table 2, temperature homogeneity achieved across the whole thermal block was very high, thanks to the specific design of the thermal block and the main lid. Second, it has been shown that the device can be used for moderate-to-high-throughput screenings, allowing the analysis of 10 species every 20 h, with an effective working time of approximately 4 h when using three devices working in parallel. Third, the equipment has proven to be capable of assessing (1) nucleation temperature; (2) the maintainability of $F_v/F_m$ after a freeze-thaw cycle at different temperatures, durations, and temperature vs. time change ramps; and (3) the time-course of $F_v/F_m$ during a freeze-thaw cycle, i.e., allowing for impact vs. recovery assessment.

As described in Table 1, the system improves the working temperature range and portability beyond the previous similar system described by Arnold et al. (2021). It also avoids the use of glass for thermal insulation of the samples, which could cause condensation and interfere with the measurements due to its reflection, transmission, or absorption coefficients in the red, blue, and NIR bands, which are the wavelength ranges in which the Imaging-PAM camera operates. Due to the specific design of the thermal block — absent in Arnold et al. (2021) device— it allows for the insertion of liquid samples, e.g., microalgae suspensions, bacteria, etc. Additionally, samples remain fully hydrated throughout the entire experimental period.

### *4.2. Freezing tolerance of PSII in Antarctic and Arctic plants*

The versatile device presented here was used to assess: (a) nucleation temperatures in a subset of Antarctic species, and (b) the monitoring of $F_v/F_m$ variation during the thermal treatment, which allows the assessment of the capacity of photosynthetic tissues to either maintain or recover $F_v/F_m$ under freeze-thaw conditions in both Antarctic and Arctic species. All these parameters have been used as indicators of species freeze-tolerance (Larcher, 2000; Pearce, 2001; Becker, Walter and Bischof, 2009; Perera-Castro et al., 2021; Petruccelli et al., 2022; Wójcik-Jagła and Rapacz, 2023; Ralser, Stegner and Neuner, 2024).

Concerning nucleation temperatures, all measures fell between −2 °C and −6 °C, well in agreement with those values compiled by Pearce (2001) and later shown for Antarctic species by Bravo et al. (2001), although they showed that values dropped to −10 °C in plants subjected to specific acclimation treatments. However, most of the studied species presented significant maintenance of $F_v/F_m$ at temperatures below the nucleation temperature. This likely indicates that ice formation occurred in the apoplast but not in the symplast, thereby preventing damage to PSII, which is located in the symplastic compartment. Thus, freezing tolerance in these species may rely on their ability to endure extracellular ice formation while maintaining symplastic integrity, possibly through the synthesis of antifreeze substances (Wanner and Junttila, 1999; Ouellet, 2007; Juurakko, diCenzo and Walker, 2021). In fact, the species with the lowest nucleation point (*P. decipiens*, Figure 4) also showed one of the lowest freezing tolerances (only second to *Desmarestia menziesii* J.Agardh, for which unfortunately no nucleation data are available). While this might suggest a trade-off between avoidance and tolerance strategies, no statistical correlation between nucleation temperature and $F_v/F_m$ maintenance was found across the dataset (Figures 4 and 5). Therefore, the pattern observed in these few species should be interpreted cautiously and considered as a hypothesis requiring further testing.

Concerning PSII tolerance below the nucleation point, some apparent phylogenetic patterns appear, although this phylogenetic approach is quite limited and applicable only to Antarctica. For instance, the present results suggest that the studied Antarctic lichens exhibit a remarkable adaptation to extremely low temperatures–which agrees with their previous reputation (Lange and Kappen, 1972; Andrzejowska et al., 2024). Lange and Kappen (1972) showed that some species recovered their photosynthesis and respiration fully after the hydrated thalli had been cooled rapidly to −196 °C. Andrzejowska et al. (2024) analyzed $F_v/F_m$ LT50 (i.e., the temperature at which $F_v/F_m$ dropped to 50 % of the initial value) in several Antarctic lichens, finding that it ranged from −16.2 °C in *Pseudophebe minuscula* to −31.9 °C in *Caloplaca regalis*, i.e., temperatures generally below those applied here. The two species they measured in common with the present study, *Usnea antarctica* Du Rietz and *Sphaerophorus globosus* (Huds.) Vain., scored LT50 of −25.3 °C and −26.6 °C, respectively (Andrzejowska et al., 2024). Bearing this in mind, further studies aiming to distinguish freezing tolerance among different lichen species should select considerably lower target temperatures. As for algae, the two studied green algae also presented strong tolerance, although this was much lower and species-dependent for red and brown algae. A remarkable freezing tolerance was also exhibited by mosses and tracheophytes, the latter both in Antarctica and in the Arctic, although much lower than that observed in lichens. Consequently, the overall data from both polar locations suggest that treatment values should be adjusted based on the phyla under study. For tracheophyte studies in polar environments, the proposed treatments to be tested next are advised to be at −6 °C, −9 °C, −12 °C, and −15 °C. For polar mosses, treatments of −8 °C, −13 °C, −18 °C, and −23 °C would be more suitable. Regarding lichens, the results indicate a need for more extreme treatments, significantly below −18 °C. For algae,

further trials with each phylum are necessary before determining appropriate experimental temperature values.

### *4.3. How does our method compare with published data on the same species?*

Besides the phylogenetic considerations and even having used progressively adapting protocols to test the new instrument, some results showed good agreement with previous reports based on completely different freezing protocols. For instance, our results show that out of the two tracheophyte species in Antarctica, *D. antarctica* tolerates freezing much better than *C. quitensis* (Figure 5). This is in full agreement with previous reports by Bravo et al. (2001, 2009) and with the completely different metabolic responses reported at non-freezing chilling temperatures (Clemente-Moreno et al., 2019, 2020). While nucleation temperature was only measured in *C. quitensis*, Bravo et al. (2001) showed that the two species presented similar values both in non-acclimated and acclimated plants to low temperature. In contrast, their freezing temperatures and, most especially, their LT50 strongly differed among the two species, the latter ranging close to −6 °C (i.e., close to the nucleation temperature) in *C. quitensis*, while ranging from −12 °C to −27 °C for non-acclimated and acclimated *D. antarctica*, respectively (Bravo et al., 2001). *D. antarctica* apoplast present anti-freezing activity while that of *C. quitensis* does not (Bravo and Griffith, 2005), while *D. antarctica* also presents ice recrystallization inhibition proteins (John et al., 2009) and a very large antioxidant activity even when non-acclimated (Bravo et al., 2009; Clemente-Moreno et al., 2020). In fact, artificial warming in the field (using open-top chambers) has been shown to reduce freezing tolerance in *C. quitensis* (Sierra-Almeida, Cavieres and Bravo, 2018) but not to a significant extent in *D. antarctica.* However, recent studies under laboratory conditions showed that increasing nocturnal warming rather than diurnal warming significantly reduced *D. antarctica* freezing tolerance, which is related to a large decrease in dehydrins and soluble carbohydrate contents (López Sanhueza, et al., 2023) and perturbation of the cold acclimation response signalling via CBF (C-repeat binding factor) regulon (López, Larama, et al., 2023). These results further support the idea that *D. antarctica* is better acclimated to low temperatures than *C. quitensis*; this is consistent with their respective distributions, *D. antarctica* being strictly peri-Antarctic, whereas *C. quitensis* ranges from Antarctica to Ecuador (GBIF, 2025a, 2025b).

Besides the differences between phylogenetic groups and between the two Antarctic tracheophytes, it seems that, in general, regarding tracheophytes, the two Antarctic species are more freezing-resistant than the Arctic species, except for *P. dahlianum*, scoring somewhat in between *D. antarctica* and *C. quitensis* (Figure 5). However, it is important to note that the highest temperature applied to Antarctic plants was −6 °C while that applied to Arctic plants was lower, −9 °C. Consequently, comparing both species is tricky except at −12 °C and −18 °C, which were common treatments. Still, when focusing on these two temperatures, *D. antarctica* was the best freezing-tolerant tracheophyte among all, *C. quitensis* staying below and at a similar range as several Arctic species, including *P. dahlianum*, but also *Bistorta vivipara* (L.) Delarbre, *D. octopetala*, *Erigeron humilis* Graham and *Poa pratensis* L. (Figure 5). Interestingly, the most freeze-tolerant Arctic species were precisely those showing a significant recovery of $F_v/F_m$ after exposure to −12 °C or −18 °C (Figure 6). None of the studied species were able to maintain a high $F_v/F_m$ during the exposure to these temperatures. As reviewed by Bravo et al. (2009), *D. antarctica* was the most freeze-tolerant tracheophyte found thus far, although close to some Alpine/Andean species like *Hordeum comosum* and *Nastanthus spathulatus*, and also to the crop winter rye (*Secale cereale)* (Bravo et al., 2009). In contrast, other Alpine/Andean species like *Poa alpina* and *Ranunculus glacialis* and also crops such as winter *Triticum aestivum* and *Hordeum vulgare*, and even some ecotypes of *Arabidopsis thaliana* reached freezing tolerances like that of *C. quitensis* (Bravo et al., 2009).

Despite the reported large variability in freezing-tolerance among and within species and varieties, there are two studies that allow direct comparison as they present results in a large number of common species to those studied here: Perera-Castro et al. (2021) for Antarctic species and Körner and Alsos (2009) for Arctic species.

Perera-Castro et al. (2021) used a standard freezer to dark-freezing Antarctic samples at –20 °C, and used $F_v/F_m$ as an indicator similarly to the present study with nine common species. *Hymenoloma crispulum* (Hedw.) Ochyra scored the highest freezing tolerance and *B. austrosalebrosum* the second in both studies, while *Syntrichia filaris* (Müll.Hal.) R.H.Zander, *Batramia patens* Brid. and *Bryum pseudotriquetrum* (Hedw.) P.Gaertn., B.Mey. & Scherb. scored the three lowest tolerances, in the same order in the two studies. *Polytrichastrum alpinum* (Hedw.) G.L.Sm., *Polytrichum piliferum* Hedw., *Sanionia uncinata* (Hedw.) Loeske and *Warnstorfia sarmentosa* (Wahlenb.) Hedenäs scored at intermediate resistances, not necessarily with the same order in both studies. Körner and Alsos (2009) also used standard freezers to dark-freezing Arctic samples at either −7 °C or −18 °C, although their observation was not based on $F_v/F_m$ but on visual symptoms and conductivity of leaf extracts. Seven of the species studied were in common with the present study. Again, there was a strong coincidence among the two studies, *P. dahlianum* being largely the most freezing-tolerant in both studies, despite having used different freezing-inducing and different evaluation methods. *D. octopetala*, one of the highlighted tolerant species in our study, was second to *P. dahlianum* in Körner and Alsos (2009) study. However, *B. vivipara* was revealed amongst the most sensitive in their study while being somewhat tolerant in ours, and the opposite happened as for *S. polaris*. Nevertheless, *Oxyria digyna* (L.) Hill, *S. cespitosa* and *Saxifraga cernua* L. scored among the less tolerant in both studies.

The very low freezing tolerance found for *S. cespitosa* and *S. cernua* in both studies, and for *Saxifraga hirculus* L. and *Saxifraga oppositifolia* L. in ours, is remarkable. Only *Saxifraga nivalis* was substantially tolerant as assessed by Körner and Alsos (2009). This is remarkable because *Saxifraga* species tolerate both high latitudes and high elevations better than any other vascular plant; *S. oppositifolia* reaches the farthest northern latitude recorded for a tracheophyte (83° 40′ N) and the highest reported elevation in Europe (>4500 m a.s.l. at the Dom summit in Switzerland) (Körner, 2011), although several tracheophyte species have been reported to reach >6100 m a.s.l. at the Western Himalayas (Angel et al., 2016; Dolezal et al., 2016; Körner, 2021). In fact, Körner and Alsos (2009) stated: 'The low freezing resistance of *S. cernua* was unexpected given that this species is common in the polar desert zone and is one of the species reaching highest up in the mountains in Svalbard'. The same claim is concerning this species and all *Saxifraga* species, especially *S. oppositifolia*. Clearly, experiments specifically dedicated to these species are necessary to disentangle the apparent mismatch between their distribution range and their low freeze-tolerance. *S. oppositifolia* has been shown to be constituted by populations with different ploidy levels (Eidesen et al., 2024), for which perhaps this can be an opportunity to explore possible explanations.

## 5. Concluding Remarks

The newly developed device effectively assesses freezing tolerance in photosynthetic tissues, demonstrating high temperature homogeneity, moderate-to-high throughput capacity, and the ability to measure multiple freezing-related parameters. Additionally, its portability and adaptability surpass previously reported systems, allowing for a broader range of experimental applications beyond freezing tolerance studies. Most studied species appear to tolerate freezing temperatures by withstanding ice formation in their apoplast. Moreover, there is a trend suggesting that species with greater freezing tolerance may maintain PSII function at temperatures below their nucleation point, while more sensitive species may tend to lower their nucleation temperature to avoid freezing damage. However, this pattern was not statistically supported across the dataset and should be interpreted as a working hypothesis requiring further investigation.

Antarctic lichens exhibit extreme freezing tolerance, while tracheophytes and algae show species-dependent variations. Comparisons between Antarctic and Arctic species indicate that Antarctic tracheophytes, particularly *D. antarctica*, are more freezing-tolerant than their Arctic counterparts, suggesting different adaptive strategies shaped by their environments.

Present results align well with previous findings, reinforcing known freezing tolerance patterns among species. However, discrepancies in freezing tolerance within the genus *Saxifraga* raise questions about other potential factors influencing freezing resistance and their relationship with plant distribution in extreme environments. In this context, the device presented constitutes a promising tool to address these questions, thanks to its portability and its ability to assess multiple freezing-related parameters, allowing for a more precise exploration of the underlying mechanisms of freezing tolerance and its variability across species, offering opportunities for future research.

## Supplementary Materials

The additional data and information can be downloaded at: https://media.sciltp.com/articles/others/250804114218715 6/plantecophys-1166-SI-final.pdf.

## Author Contributions

FC-M directed the development of the device, its implementation in the experiments and wrote the manuscript. JG conceived the idea, designed experiments and supervised manuscript. MR helped write the manuscript. The remaining authors assisted in some experiments, and all authors contributed to the final version of the manuscript. All authors have read and agreed to the published version of the manuscript.

## Funding

This work was supported by the project POPEYE, PID2022-139455NB-C31, PID2022-139455NB-C32 and EREMITA PGC2018-093824-B-C41, PGC2018-093824-B-C43, PGC2018-093824-B-C44, from Ministerio de Ministerio de Ciencia, Innovación y Universidades (MICIU, Spain), European Regional Development Fund (ERDF) and Agencia Estatal de Investigación (AEI, Spain). F. Castanyer-Mallol was supported by a predoctoral fellowship PRE2019-090011 from MINECO and AEI. JM-A and EN-O acknowledge funding by PID2023-150695NB-I00, funded by MCIU/AEI/10.13039/501100011033/FEDER, UE. MC was supported by a Vicenç Mut 2022 postdoctoral fellowship (PD-047-2022) funded by Conselleria de Fons Europeus, Universitat i Cultura from Govern de les Illes Balears. BFM enjoyed the RYC2021-031321-I grant funded by MCIN/AEI/10.13039/501100011033 and by the European Union Next-GenerationEU/PRTR.

## Data Availability Statement

The datasets used and/or analyzed during the current study are available from the corresponding author on reasonable request.

## Acknowledgments

These results have been partially obtained at the 'Spanish Antarctic Station Juan Carlos I' after having accessed during the 2021–2022 Spanish Antarctic Campaign. The extraordinary support received at the BAE JCI Station and during the campaign from the 'Unidad de Tecnología Marina-UTM' and the 'Comité Polar Español CPE' is also deeply acknowledged, with special mention to Joan Riba because of his positive attitude and troubleshooting capability along the whole campaign. We would also like to thank Prof. Mike McCagon for his extensive English correction of the manuscript.

## Conflicts of Interest

Francesc Castanyer-Mallol is the inventor of both the national and international patents (ES 2 960 435 A1 and WO/2024/028532 A1), which cover the thermoelectric device described in this manuscript. The other authors declare no competing interests.

## Peer Review Statement

Plant Ecophysiology acknowledges the contributions of two anonymous reviewers to the peer review of this manuscript.

## References


Adhikari L, Baral R, Paudel D, Min D, Makaju SO, Poudel HP, & Missaoui AM. (2022). Cold stress in plants: Strategies to improve cold tolerance in forage species. *Plant Stress*, *4*, 100081. https://doi.org/10.1016/J.STRESS.2022.100081.

Andrzejowska A, Hájek J, Puhovkin A, Harańczyk H, & Barták M. (2024). Freezing temperature effects on photosystem II in Antarctic lichens evaluated by chlorophyll fluorescence. *Journal of Plant Physiology*, *294*, 154192. https://doi.org/10.1016/j.jplph.2024.154192.

Angel R, Conrad R, Dvorsky M, Kopecky M, Kotilínek M, Hiiesalu I, & Doležal J. (2016). The Root-Associated Microbial Community of the World's Highest Growing Vascular Plants. *Microbial Ecology*, *72*(2), 394–406. https://doi.org/10.1007/s00248-016-0779-8.

Arnold PA, Briceño VF, Gowland KM, Catling AA, Bravo LA, & Nicotra AB. (2021). A high-throughput method for measuring critical thermal limits of leaves by chlorophyll imaging fluorescence. *Functional Plant Biology*, *48*(6), 634–646. https://doi.org/10.1071/FP20344.

Arzac Garmendia MI, Miranda González de Apodaca J, De los Ríos A, Castanyer Mallol F, García Plazaola JI, & Fernández Marín B. (2024). The outstanding capacity of *Prasiola antarctica* to thrive in contrasting harsh environments relies on the constitutive protection of thylakoids and on morphological plasticity. *The Plant Journal*, *119*(1), 65–83. https://doi.org/10.1111/tpj.16742.

Becker S, Walter B, & Bischof K. (2009). Freezing tolerance and photosynthetic performance of polar seaweeds at low temperatures. *Botanica Marina*, *52*(6), 609–616. https://doi.org/10.1515/BOT.2009.079.

Birkeland S, Slotte T, Krag Brysting A, Gustafsson AL S, Rhoden Hvidsten T, Brochmann C, & Nowak MD. (2022). What can cold-induced transcriptomes of Arctic Brassicaceae tell us about the evolution of cold tolerance? *Molecular Ecology*, *31*(16), 4271–4285. https://doi.org/10.1111/mec.16581.

Bravo LA, & Griffith M. (2005). Characterization of antifreeze activity in Antarctic plants. *Journal of Experimental Botany*, *56*(414), 1189–1196. https://doi.org/10.1093/jxb/eri112.

Bravo LA, Ulloa N, Zuñiga GE, Casanova A, Corcuera LJ, & Alberdi M. (2001). Cold resistance in Antarctic angiosperms. *Physiologia Plantarum*, *111*, 55–65. https://doi.org/10.1034/j.1399-3054.2001.1110108.x.

Bravo LA, Bascuñán-Godoy L, Pérez-Torres E, & Corcuera LJ. (2009). Cold Hardiness in Antarctic Vascular Plants. In *Plant cold hardiness: From the laboratory to the field*. (Gusta LV, Wisniewski ME, Tanino KK, Eds.) (p. 317). CABI.

Chaudhary S, Devi P, Bhardwaj A, Jha UC, Sharma KD, Prasad PV, & Nayyar H. (2020). Identification and Characterization of Contrasting Genotypes/Cultivars for Developing Heat Tolerance in Agricultural Crops: Current Status and Prospects. *Frontiers in Plant Science*, *11*, 587264. https://doi.org/10.3389/fpls.2020.587264.

Clemente-Moreno MJ, Omranian N, Sáez P, Figueroa CM, Del-Saz N, Elso M, & Gago J. (2019). Cytochrome respiration pathway and sulphur metabolism sustain stress tolerance to low temperature in the Antarctic species Colobanthus quitensis. *New Phytologist*, *225*(2), 754–768. https://doi.org/10.1111/nph.16167.

Clemente-Moreno MJ, Omranian N, Sáez PL, Figueroa CM, Del-Saz N, Elso M, & Gago J. (2020). Low-temperature tolerance of the Antarctic species Deschampsia antarctica: A complex metabolic response associated with nutrient remobilization. *Plant Cell and Environment*, *43*(6), 1376–1393. https://doi.org/10.1111/pce.13737.

Danzey LM, Briceño VF, Cook AM, Nicotra AB, Peyre G, Rossetto M, & Leigh A. (2024). Environmental and Biogeographic Drivers behind Alpine Plant Thermal Tolerance and Genetic Variation. *Plants*, *13*(9), 1271. https://doi.org/10.3390/plants13091271.

De Mendiburu F. (2021). *agricolae: Statistical procedures for agricultural research*. R package version 1.3-5. https://CRAN.R-project.org/package=agricolae.

Dolezal J, Dvorsky M, Kopecky M, Liancourt P, Hiiesalu I, Macek M, & Schweingruber F. (2016). Vegetation dynamics at the upper elevational limit of vascular plants in Himalaya. *Scientific Reports*, *6*, 24881. https://doi.org/10.1038/srep24881.

Eidesen PB, Brysting AK, Hagen KR, Hjelle SS, Reveret A, Tjessem IV, & Volden IK. (2024). Ecological and evolutionary consequences of ploidy-driven trait variation: Insights from Saxifraga oppositifolia L. *Arctic Science*, *11*, 1–26. https://doi.org/10.1139/as-2024-0020.

Fernández-Marín B, Gulías J, Figueroa CM, Iñiguez C, Clemente-Moreno MJ, Nunes-Nesi A, & Gago J. (2020). How do vascular plants perform photosynthesis in extreme environments? An integrative ecophysiological and biochemical story. *Plant Journal*, *101*(4), 979–1000. https://doi.org/10.1111/tpj.14694.

Flexas J, Fernie AR, Usadel B, Alonso-Forn D, Ardiles V, Ball MC, & Gago J. (2025). What can we learn from the ecophysiology of plants inhabiting extreme environments? from 'sherplants' to 'shercrops'. *Journal of Experimental Botany*, Eraf236. https://doi.org/10.1093/jxb/eraf236

Fox J, & Weisberg S. (2019). *Car: Companion to applied regression*. R package version 3.0-10. https://CRAN.R-project.org/package=car.

GBIF. (2025a, April 17). *GBIF Backbone taxonomy*: *Deschampsia antarctica* É. Desv. Checklist dataset. https://www.gbif.org/species/4144844.

GBIF. (2025b, April 17). *GBIF Backbone taxonomy*: *Colobanthus quitensis* (Kunth) Bartl. Checklist dataset. https://www.gbif.org/species/5588218.

Geange SR, Arnold PA, Catling AA, Coast O, Cook AM, Gowland KM, & Nicotra AB. (2021). The thermal tolerance of photosynthetic tissues: a global systematic review and agenda for future research. *New Phytologist*, *229*, 2497–2513. https://doi.org/10.1111/nph.17052.

Graves S, Piepho HP, Selzer L, & Dorai-Raj S. (2019). *multcompView: Visualizations of paired comparisons*. R package version 0.1-8. https://CRAN.R-project.org/package=multcompView.

Harris RJ, Bryant C, Coleman MA, Leigh A, Briceño VF, Arnold PA, & Nicotra AB. (2023). A novel and high-throughput approach to assess photosynthetic thermal tolerance of kelp using chlorophyll α fluorometry. *Journal of Phycology*, *59*(1), 179–192. https://doi.org/10.1111/jpy.13296.

Hothorn T, Bretz F, & Westfall P. (2008). *multcomp: Simultaneous inference in general parametric models*. R package version 1.4-25. https://CRAN.R-project.org/package=multcomp.

John UP, Polotnianka RM, Sivakumaran KA, Chew O, Mackin L, Kuiper MJ, & Spangenberg GC. (2009). Ice recrystallization inhibition proteins (IRIPs) and freeze tolerance in the cryophilic Antarctic hair grass *Deschampsia antarctica* E. Desv. *Plant, Cell and Environment*, *32*(4), 336–348. https://doi.org/10.1111/j.1365-3040.2009.01925.x.

Junttila O, & Robberecht R. (1993). The Influence of Season and Phenology on Freezing Tolerance in Silene acaulis L., a Subarctic and Arctic Cushion Plant of Circumpolar Distribution. *Annals of Botany*, *71*, 423–426. https://doi.org/10.1006/anbo.1993.1054.

Juurakko CL, diCenzo GC, & Walker VK. (2021). Cold acclimation and prospects for cold-resilient crops. *Plant Stress*, *2*, 100028. https://doi.org/10.1016/j.stress.2021.100028.

Körner C. (2011). Coldest places on earth with angiosperm plant life. *Alpine Botany*, *121*(1), 11–22. https://doi.org/10.1007/s00035-011-0089-1

Körner C. (2021). Climatic stress. In *Alpine plant life* (pp. 175–201). Springer. https://doi.org/10.1007/978-3-030-59538-8_8.

Körner C, & Alsos IG. (2009). Freezing resistance in high arctic plant species of Svalbard in mid-summer. *Bauhinia*, *21*, pp. 25–32. https://www.researchgate.net/publication/242389283.

Lange OL, & Kappen L. (1972). Photosynthesis of Lichens from Antarctica. In *Antarctic terrestrial biology* (Llano GA. Ed.) (pp. 83–96). American Geophysical Union.

Larcher W. (2000). Temperature stress and survival ability of mediterranean sclerophyllous plants. *Plant Biosystems*, *134*(3), 279–295. https://doi.org/10.1080/11263500012331350455.

Lenth RV. (2023). *emmeans: Estimated marginal means, aka least-squares means*. R package version 1.8.9. https://CRAN.R-project.org/package=emmeans.

Li H, Wang Z, Yu Y, Gao W, Zhu J, Zhang H, & Liu Y. (2024). Enhancing cold tolerance in tobacco through endophytic symbiosis with Piriformospora indica. *Frontiers in Plant Science*, *15*, 1459882. https://doi.org/10.3389/FPLS.2024.1459882.

López D, Larama G, Sáez PL, & Bravo LA. (2023). Transcriptome Analysis of Diurnal and Nocturnal-Warmed Plants, the Molecular Mechanism Underlying Cold Deacclimation Response in Deschampsia antarctica. *International Journal of Molecular Sciences*, *24*(13). https://doi.org/10.3390/ijms241311211.

López D, Sanhueza C, Salvo-Garrido H, Bascunan-Godoy L, & Bravo LA. (2023). How Does Diurnal and Nocturnal Warming Affect the Freezing Resistance of Antarctic Vascular Plants? *Plants*, *12*(4). https://doi.org/10.3390/plants12040806.

López-Pozo M, Flexas J, Gulías J, Carriquí M, Nadal M, Perera-Castro AV, & Fernández-Marín B. (2019). A field portable method for the semi-quantitative estimation of dehydration tolerance of photosynthetic tissues across distantly related land plants. *Physiologia Plantarum*, *167*(4), 540–555. https://doi.org/10.1111/ppl.12890.

Maxwell K, & Johnson GN. (2000). Chlorophyll fluorescence—a practical guide. *Journal of Experimental Botany*, *51*(345), 669–668. https://doi.org/10.1093/jxb/51.345.659.

Norman PA, Huner GÖ, & Fathey S. (1998). Energy balance and acclimation to light and cold. *Trends in Plant Science*, *3*(6), 224–230. https://doi.org/10.1016/S1360-1385(98)01248-5.

Ouellet F. (2007). Cold Acclimation and Freezing Tolerance in Plants. In *Encyclopedia of life sciences*. Wiley. https://doi.org/10.1002/9780470015902.a0020093.

Paulsen G. (2002). Application of Physiology in Wheat Breeding. *Crop Science*, *42*(6), 2228–2229. https://doi.org/10.2135/cropsci2002.2228.

Pearce RS. (2001). Plant freezing and damage. In *Annals of botany* (pp. 417–424). Academic Press. https://doi.org/10.1006/anbo.2000.1352.

Peat HJ, Clarke A, & Convey P. (2007). Diversity and biogeography of the Antarctic flora. *Journal of Biogeography*, *34*(1), 132–146. https://doi.org/10.1111/j.1365-2699.2006.01565.x.

Perera-Castro AV, Brito P, & González-Rodríguez AM. (2018). Changes in thermic limits and acclimation assessment for an alpine plant by chlorophyll fluorescence analysis: $F_v/F_m$ vs. Rfd'. *Photosynthetica, 56*, 527–536. https://doi.org/10.1007/s11099-017-0691-6.

Perera-Castro AV, Flexas J, González-Rodríguez ÁM, & Fernández-Marín B. (2021). Photosynthesis on the edge: photoinhibition, desiccation and freezing tolerance of Antarctic bryophytes. *Photosynthesis Research*, *149*, 135–153. https://doi.org/10.1007/s11120-020-00785-0.

Petruccelli R, Bartolini G, Ganino T, Zelasco S, Lombardo L, Perri E, & Bernardi R. (2022). Cold Stress, Freezing Adaptation, Varietal Susceptibility of *Olea europaea* L.: A Review. *Plants*, *11*(10), 1367. https://doi.org/10.3390/plants11101367.

Pinheiro J, Bates D, DebRoy S, Sarkar D, & R Core Team. (2023). *nlme: Linear and nonlinear mixed effects models*. R package version 3.1-162. https://CRAN.R-project.org/package=nlme.

Ralser M, Stegner M, & Neuner G. (2024). When water turns to ice: Control of ice volume and freezing dynamics as important aspects of cold acclimation. *Environmental and Experimental Botany*, *227*, 105957. https://doi.org/10.1016/j.envexpbot.2024.105957.

Robberecht R, & Junttila O. (1992). The Freezing Response of an Arctic Cushion Plant, Saxifraga caespitosa L.: Acclimation, Freezing Tolerance and Ice Nucleation. *Annals of Botany*, *70*(2), 129–135. https://doi.org/10.1093/oxfordjournals.aob.a088449.

Sakai A, & Larcher W. (1987). *Frost Survival of Plants, Responses and Adaptation to Freezing Stress* (Durham WDB, Athens FG, Würzburg OLL, Oak Ridge JSO, Merburg HR, Eds.). Springer-Verlag. https://archive.org/details/frostsurvivalofoO000saka

Sierra-Almeida A, Cavieres LA, & Bravo LA. (2018). Warmer temperatures affect the in situ freezing resistance of the antarctic vascular plants. *Frontiers in Plant Science*, *9*, 1456. https://doi.org/10.3389/fpls.2018.01456.

Stange R. (2018). Spitsbergen-Svalbard. In *The complete guidebook around the arctic archipelago* (4th ed.). Rolf.

Thalhammer A, & Hincha DK. (2014). A mechanistic model of COR15 protein function in plant freezing tolerance: Integration of structural and functional characteristics. *Plant Signaling and Behavior*, *9*(12), e977722–e977723. https://doi.org/10.4161/15592324.2014.977722.

Wang C, Zhang M, Zhou J, Gao X, Zhu S, Yuan L, & Hou J. (2022). Transcriptome analysis and differential gene expression profiling of wucai (*Brassica campestris* L.) in response to cold stress. *BMC Genomics*, *23*(1), 137. https://doi.org/10.1186/s12864-022-08311-3.

Wanner LA, & Junttila O. (1999). Cold-Induced Freezing Tolerance in Arabidopsis. *Plant Physiology*, *120*, 391–399. https://doi.org/10.1104/pp.120.2.391.

Wienckel C, & tom Dieck I. (1990). Temperature requirements for growth and survival of macroalgae from Antarctica and southern Chile. *Marine Ecology Progress Series*, 59, 157–170. http://www.jstor.org/stable/24837833.

Wójcik-Jagła M, & Rapacz M. (2023). Freezing tolerance and tolerance to de-acclimation of European accessions of winter and facultative barley. *Scientific Reports*, *13*(1), 19931. https://doi.org/10.1038/s41598-023-47318-y.